In vivo leukocyte imaging: Palestro reviews methods under development for and challenges to in vivo labeling of leukocytes that migrate to sites of infection and previews an article in this month's *JNM* on the utility of interleukin-8 in these investigations. . . . . ***Page 332***

Right answers, right reasons: Porenta looks at the role of formal, rule-based "expert systems" in knowledge processing and problem solving, with specific reference to an article in this month's *JNM* on the application of such a system in diuresis nephrography. . . . . ***Page 335***

Targeting infection: Bleeker-Rovers and colleagues evaluate the safety of interleukin-8 (IL-8) in humans and assess the value of ^{99m}Tc-IL-8 scintigraphy in patients with suspected localized infections. . . . . ***Page 337***

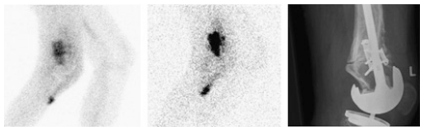

Cardiac risk and cancer: Chang and colleagues compare the incidence of perioperative cardiac events in cancer patients who have previous abnormal stress myocardial perfusion imaging (MPI) results with that in cancer patients whose MPI results were normal. . . . . ***Page 344***

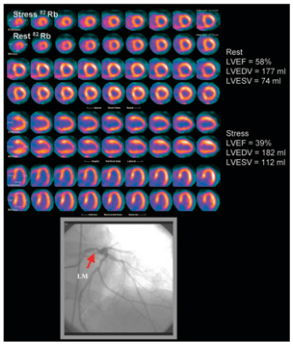

Excluding multivessel CAD: Dorbala and colleagues use ^{82}Rb-PET to investigate the value of vasodilator left ventricular ejection fraction reserve in determining both the magnitude of myocardium at risk and the anatomic extent of underlying coronary artery disease. . . . . ***Page 349***

SPECT brain tracer binding: Booij and colleagues report on the influence of paroxetine, a selective serotonin reuptake inhibitor, on ^{123}I-FP-CIT binding to dopamine transporter in the healthy striatum. . . .***Page 359***

PET and soft-tissue sarcoma: Been and colleagues use ^{18}F-FLT PET to measure responses to hyperthermic isolated limb perfusion treatment in patients with primary soft-tissue sarcomas in the extremities and discuss the benefits for surgical planning. . . . . ***Page 367***

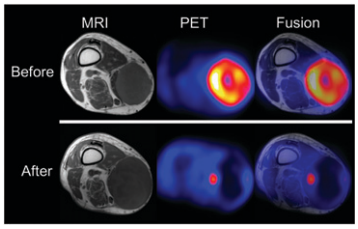

PET assesses early RT response: Kim and colleagues evaluate the predictive efficacy of ^{18}F-FDG PET imaging acquired 1 month after completion of radiotherapy in patients with squamous cell carcinoma of the head and neck. . . . . ***Page 373***

Thryotoxicosis overview: Iagaru and McDougall provide a comprehensive educational review of thyrotoxicosis, including causes, diagnosis, and the benefits and potential side effects of the 3 most common treatment approaches: antithyroid medications, surgical thyroidectomy, and ^{131}I administration. . . . . ***Page 379***

Clarifying posttreatment PET: Brepoels and colleagues investigate whether posttherapeutic tumor inflammation can be suppressed by administration of corticosteroids and thereby improve accurate correlation of ^{18}F-FDG uptake with tumor cell kill. . . . . ***Page 390***

Advancing gene therapy: Lim and colleagues explore the effect of retinoic acid on adenovirus-mediated expression of the human sodium iodide symporter gene in a breast cancer cell line. . . . . ***Page 398***

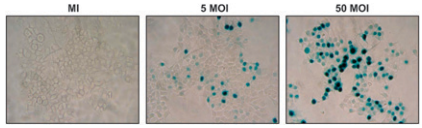

SPECT and stem cell therapy: Tran and colleagues describe an original pinhole SPECT technique in a rat model of myocardial infarction and analyze local improvement in myocardial perfusion after engraftment of bone marrow–derived stem cells. . .***Page 405***

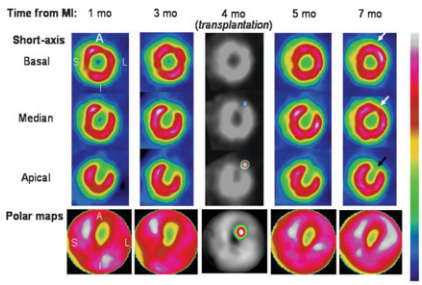

Acute responses to smoke inhalation: Schroeder and colleagues test whether cigarette smoke–related PET imaging changes in regional intrapulmonary distribution of ^{18}F-FDG uptake in a sheep model are related to changes in regional lung function as assessed with infused ^{13}NN-saline. . . . . ***Page 413***

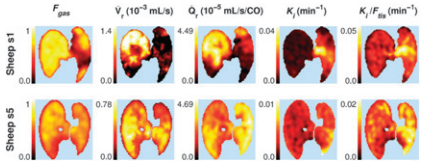

^{18}F-FAC for tumor imaging: Ponde and colleagues radiosynthesize ^{18}F-fluoroacetate, perform biodistribution studies in rats and mice, and assess the potential usefulness of this tracer as an alternative to ^{11}C-ACE for PET detection of prostate tumors. . . . . ***Page 420***

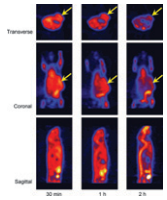

Two-step tumor imaging with phage: Newton and colleagues explore the use of a multivalent bifunctional phage displaying peptides that target novel molecular biomarkers to facilitate pretargeting and subsequent imaging of murine melanoma in vivo. . . . . ***Page 429***

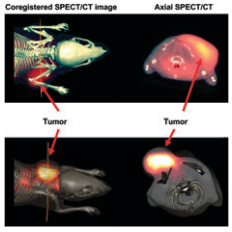

Thermal dosimetry as predictor: DeNardo and colleagues use nanoparticle bioprobes to evaluate tumor targeting, efficacy, and predictive radionuclide-based heat dosimetry of tumor-specific thermal therapy in a human breast cancer xenograft model. . . . . ***Page 437***

Imaging antiangiogenic effects: Hsu et al. study the antiangiogenic and antitumor efficacy of vascular-targeting fusion toxin VEGF$_{121}$/rGel in an orthotopic glioblastoma mouse model using in vivo bioluminescence imaging, MRI, and PET. . . . . ***Page 445***

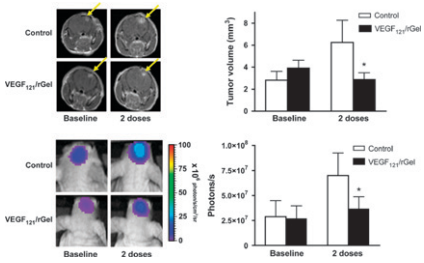

Fatty acid analog for PET: Guiducci and colleagues describe the biodistribution and partitioning of ^{18}F-FTHA, a fatty acid analog, across different lipid pools in plasma and in metabolically important organs and assess its response to insulin. . . . . ***Page 455***

Automating diagnostic accuracy: Garcia and colleagues evaluate the inference engine of an "expert system" that generates explanations of the reasoning process for diagnosing renal obstruction from diuresis renography. . . . . ***Page 463***

3D, time-of-flight PET: Surti and colleagues report performance results from a fully 3D-mode PET/CT scanner that uses lutetium-yttrium oxyorthosilicate crystals for the PET component and achieves time-of-flight imaging without sacrificing conventional PET or CT capabilities. . . . . ***Page 471***

Low-dose ^{131}I thyroid stunning: Lundh and colleagues investigate the effects of ^{131}I irradiation on ^{125}I transport and cell proliferation at low absorbed doses in vitro. . . . . ***Page 481***

Ultra-high-resolution SPECT: Vastenhouw and Beekman describe a combined acquisition and reconstruction strategy for whole-body mouse imaging using a new stationary SPECT system dedicated to small-animal imaging. . . . . ***Page 487***

ON THE COVER

Bioprobes are monoclonal antibody–equipped nanoparticles that, when given systemically, can reach and bind to tumor cells and provide a new way to direct thermal ablation specifically to those cells via external application of an alternating magnetic field. ^{111}In-Bioprobes containing iron oxide have been shown effective in targeting human breast cancer xenografts in mice. Radionuclide concentration enabled calculation of total heat doses that were predictive of tumor response achieved without toxicity.

SEE PAGE 438